New Redox-Active Iron(II) Acetylide Complex Bearing a (2-Pyridyl)aldimine Site. Synthesis and Complexation to Copper(I)

Safaa Ibn Ghazala,[†] Nicolas Gauthier,[†] Frédéric Paul,*[,†] Loic Toupet,[‡] and Claude Lapinte*[,†]

Sciences Chimiques de Rennes, Université de Rennes I, CNRS (UMR 6226), Campus de Beaulieu, Bâtiment 10C, 35042 Rennes Cedex, France, and Groupe Matière Condensée et Matériaux, Université de Rennes I, CNRS (UMR 6626), Campus de Beaulieu, 35042 Rennes Cedex, France

Received November 29, 2006

We report in this contribution the isolation and characterization of a new redox-active "(η^2-dppe)(η^5-C_5Me_5)FeC≡C-4-(C_6H_4)−" complex bearing a (2-pyridyl)aldimine site on the aryl ring. This new metallo ligand, which was isolated by an unusual synthetic route from the known amino precursor complex, was structurally characterized. In accord with its "metallo ligand" denomination, we show here that it readily reacts with several Cu(I) precursors to form selectively, in good yields, complexes similar to those obtained with the corresponding organic *N*-aryl-(2-pyridyl)aldimines. By this method, a new dinuclear Fe(II)/Cu(I) complex and a new trinuclear Fe(II)/Cu(I)/Fe(II) complex were obtained in a straightforward way and characterized. The solid-state structure of the latter complex was also determined. Subsequently, the redox congeners of these closed-shell compounds were generated in situ by oxidation and the electronic structures of the open-shell parents were briefly investigated by infrared, ESR, and UV/vis spectroelectrochemistry. For instance, we conclusively show here that the mixed-valent (MV) state of the trinuclear complex belongs to class I in the classification of Robin and Day.

Introduction

Judicious spatial or topologic organization of redox-active end groups can lead to molecular architectures presenting unique properties for information storage or information processing at the molecular level.[1] Accordingly, this area constitutes the center of active research from various groups involved in molecular-based electronics around the world.[2] In this connection, we have shown in several instances over the last 10 years that the "(η^2-dppe)(η^5-C_5Me_5)FeC≡C−" fragment can impart interesting properties to various carbon-rich architectures.[3] The resulting polynuclear assemblies proved usually to be stable (and isolable) in different redox states and most often exhibited quite appealing performances in the realization of molecular-based devices such as molecular wires, molecular diodes, and molecular magnets.[4−6] Moreover, the available Fe(II) precursors of this remarkable organoiron fragment present a versatile coupling chemistry which allows its introduction into carbon-rich architectures by forming covalent Fe−C or C−C bonds.[7,8]

The isolation of ubiquitous ligating units functionalized with this redox-active organoiron end group would open even more possibilities to achieve various topologic organizations of this particular redox center in space, using simple coordination reactions with different templating metal cations. Following this approach, we have previously reported the synthesis of compounds such as **1a**−**c** (Chart 1), bearing a pyridine coordination site, along with some coordination reactions of these new

* To whom correspondence should be addressed. E-mail: frederic.paul@univ-rennes1.fr (F.P.); claude.lapinte@univ-rennes1.fr (C.L.).

[†] Sciences Chimiques de Rennes, Université de Rennes I. Tél: (33) 02 23 23 59 62. Fax: (33) 02 23 23 56 37.

[‡] Groupe Matière Condensée et Matériaux, Université de Rennes I. Tél: (33) 02 23 23 64 97. Fax: (33) 02 23 23 52 92.

(1) (a) Balzani, V.; de Silva, A. P. *Electron Transfer in Chemistry*; Wiley-VCH, Weinheim, Germany, 2000; Vol. 5. Norgaard, K.; Bjornholm, T. *Chem. Commun.* **2005**, 1812−1823. (b) Gianneschi, N. C.; Masar, M. S., III; Mirkin, C. A. *Acc. Chem. Res.* **2005**, *38*, 825−837. (c) Lehn, J.-M. *Angew. Chem., Int. Ed. Engl.* **1990**, *29*, 1304−1319. (d) Lehn, J. M. *Supramolecular. Chemistry-Concepts and Perspectives*; VCH: Weinheim, Germany, 1995.

(2) For contributions concerned with carbon-rich organometallics, see for instance: (a) Coe, B. J. *Acc. Chem. Res.* **2006**, *39*, 383−393. (b) Wong, C.-Y.; Tong, G. S. M.; Che, C.-M.; Zhu, N. *Angew. Chem., Int. Ed.* **2006**, *45*, 2694−2698. (c) Cordiner, R. L.; Smith, M. E.; Batsanov, A. S.; Albesa-Jové, D.; Hartl, F.; Howard, J. A. K.; Low, P. J. *Inorg. Chim. Acta* **2006**, *359*, 946−961. (d) Qi, H.; Ghupta, A.; Noll, B. C.; Snider, G. L.; Lu, Y.; Lent, C. S.; Fehlner, T. P. *J. Am. Chem. Soc.* **2005**, *127*, 15218−15227. (e) Jiao, J.; Long, G. J.; Rebbouh, L.; Grandjean, F.; Beatty, A. M.; Fehlner, T. P. *J. Am. Chem. Soc.* **2005**, *127*, 17819−17831. (f) Kheradmandan, S.; Venkatesan, K.; Blacque, O.; Schmalle, H.; Berke, H. *Chem. Eur. J.* **2004**, *10*, 4872−4885. (g) Venkatesan, K.; Blacque, O.; Fox, T.; Alfonso, M.; Schmalle, H. W.; Kheradmandan, S.; Berke, H. *Organometallics* **2005**, *24*, 920−932. (h) Venkatesan, K.; Blacque, O.; Berke, H. *Organometallics* **2006**, *25*, 5190−5200. (i) Ren, T. *Organometallics* **2005**, *24*, 4854−4870. (j) Kühn, F. E.; Zuo, J.-L.; de Biani, F. F.; Santos, A. M.; Zhang, Y.; Zhao, J.; Sandulache, A.; Herdtweck, E. *New J. Chem.* **2004**, *28*, 43−51. (k) Lindner, E.; Zong, R.; Eichele, K.; Ströbele, M. *J. Organomet. Chem.* **2002**, *660*, 78−84. (l) Sheng, T.; Vahrenkamp, H. *Eur. J. Inorg. Chem.* **2004**, 1198−1203. (m) Ziessel, R. *Synthesis* **1999**, 1839−1865.

(3) (a) Ibn Ghazala, S.; Paul, F.; Toupet, L.; Roisnel, T.; Hapiot, P.; Lapinte, C. *J. Am. Chem. Soc.* **2006**, *128*, 2463−2476. (b) Shaw-Taberlet, J. A.; Sinbandhit, S.; Roisnel, T.; Hamon, J.-R.; Lapinte, C. *Organometallics* **2006**, *25*, 5311−5325. (c) Samoc, M.; Gauthier, N.; Cifuentes, M. P.; Paul, F.; Lapinte, C. *Angew. Chem., Int. Ed.* **2006**, *45*, 7376−7379. (d) de Montigny, F.; Argouarch, G.; Costuas, K.; Halet, J.-F.; Roisnel, T.; Toupet, L.; Lapinte, C. *Organometallics* **2005**, *24*, 4558−4572. (e) Bruce, M.; Costuas, K.; Davin, T.; Ellis, B. J.; Halet, J.-F.; Lapinte, C.; Low, P. J.; Smith, M. E.; Skelton, B. W.; Toupet, L.; White, A. H. *Organometallics* **2005**, *24*, 3864−3881.

(4) Jiao, H.; Gladysz, J. A.; Costuas, K.; Halet, J.-F.; Toupet, L.; Paul, F.; Lapinte, C. *J. Am. Chem. Soc.* **2003**, *125*, 9511−9522.

(5) Paul, F.; Lapinte, C. In *Unusual Structures and Physical Properties in Organometallic Chemistry*; Gielen, M., Willem, R., Wrackmeyer, B., Eds.; Wiley: San Francisco, 2002; pp 219−295.

(6) Paul, F.; Lapinte, C. *Coord. Chem. Rev.* **1998**, *178/180*, 427−505.

(7) Courmarcel, J.; Le Gland, G.; Toupet, L.; Paul, F.; Lapinte, C. *J. Organomet. Chem.* **2003**, *670*, 108−122.

(8) (a) Denis, R.; Weyland, T.; Paul, F.; Lapinte, C. *J. Organomet. Chem.* **1997**, *545/546*, 615−618. (b) Le Stang, S.; Lenz, D.; Paul, F.; Lapinte, C. *J. Organomet. Chem.* **1998**, *572*, 189−192.

10.1021/om061081w CCC: $37.00
Publication on Web 03/29/2007

Chart 1

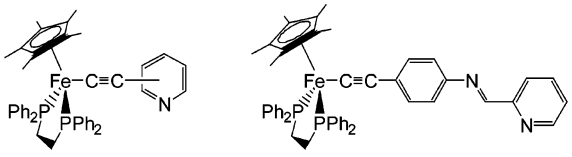

1a-c **2**

Scheme 1

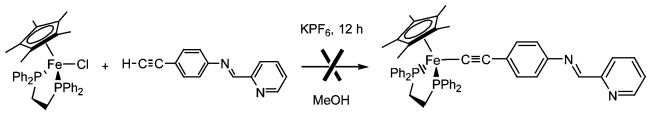

4 **3** **2**

Scheme 2

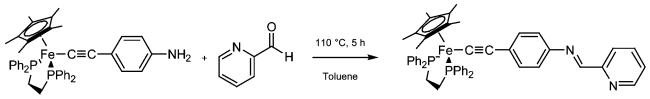

5 **6** **2**

organometallic ligands with various metal centers. However, these metallo ligands proved quite labile in some complexes, undergoing spontaneous decoordination in coordinating solvents or in the presence of competing ligands.[9,10] This phenomenon was detrimental to their use as molecular precursors of the "(η^2-dppe)(η^5-C_5Me_5)FeC≡C−" fragment, and the synthesis of similar metallo ligands bearing a polytopic chelating site was envisioned to overcome this limitation. Indeed, chelating polypyridyl ligands are well-known to present affinities for Lewis acidic centers greater than those of their single-site relatives. Unfortunately, our first attempts at isolating analogues of **1a**−**c** bearing a bipyridine fragment instead of the pyridyl site were not successful.[11] We therefore targeted Fe(II) acetylide complexes featuring other diimine-like complexing units. The present paper describes our first attempt toward this goal, using the *N*-aryl(2-pyridyl)aldimine moiety. Accordingly, we report in the following (i) the synthesis and characterization of the new redox-active metallo ligand **2**, featuring a (2-pyridyl)-aldimine site, (ii) some reactions of this compound with Cu(I) precursors, and (iii) a brief study of the oxidized parents of **2** and of the new heteropolymetallic complexes isolated.

Results

Synthesis and Characterization of the New Metallo Ligand 2. We initally attempted to isolate the target compound **2** from the presynthesized alkyne **3** and the iron chloride precursor **4**, using the well-known activation reaction operative in the presence of KPF_6 in methanol (Scheme 1).[6] However, as previously observed when 2,2′-diethynylbipyridine derivatives were used instead of **3**,[11] this reaction proved unselective and led to mixtures of unidentified compounds. We therefore devised another synthetic route to obtain the desired compound **2**.

The synthesis of **2** was subsequently attempted by starting from the known *p*-amino complex **5**.[12] The latter was reacted with 2-pyridinecarboxaldehyde (**6**) in methanol or toluene with heating.[13,14] Regardless of the solvent used, the reaction worked well and the desired complex **2** was obtained with comparable yield (71−74%) each time. The synthesis in toluene was preferred, since it occurred more quickly in this solvent, which allowed for stronger heating (Scheme 2).

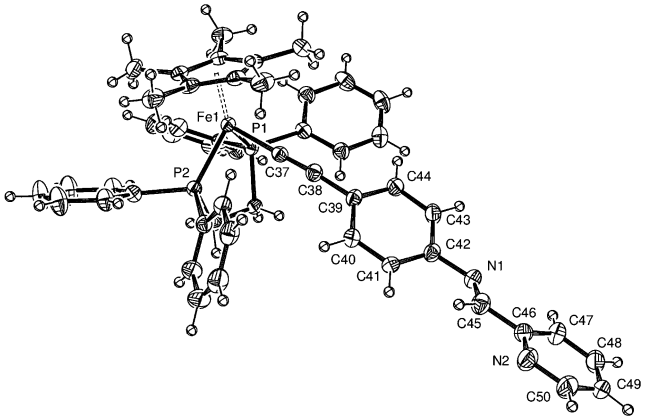

Figure 1. ORTEP representation of the diimine complex **2** at the 50% probability level.

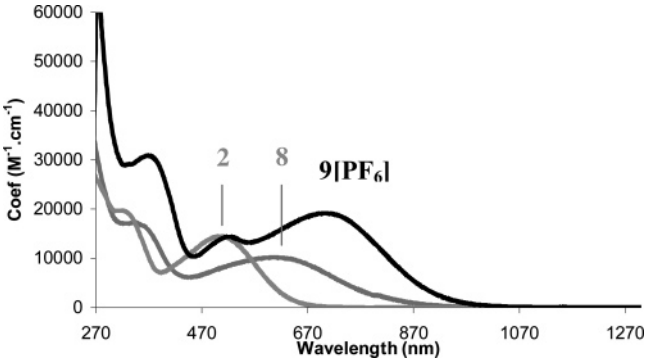

Figure 2. UV−vis spectra for **2**, **8**, and **9**[PF_6] in dichloromethane.

The desired orange-red organometallic diimine complex **2** was isolated by precipitation and characterized according to the usual spectroscopic techniques and by FAB-MS. Unfortunately, we were unable to obtain an accurate elemental analysis of this compound, probably due to the slow evaporation of dichloromethane solvate molecules and a larger amount of solvent in the microcrystals than in single crystals (see X-ray analysis). Small garnet red crystals could be grown, however, by slow diffusion of *n*-pentane into a dichloromethane solution of the complex (see below), and the solid-state structure was obtained (Figure 1). In addition, the adduct of **2** with a cuprous salt provides the analytically pure complex **9**[PF_6] (vide infra).

The purity of the isolated product can be ascertained by the observation of a single new peak at 101.4 ppm in ^{31}P NMR, while both ^1H and ^{13}C NMR reveal the presence of a single set of signals corresponding to one complex, in line with the regioselective formation of the (*E*)-diimine isomer characterized by X-ray studies. The observation of a strong $\nu_{C\equiv C}$ stretch in the infrared region near 2045 cm^{-1} is diagnostic of the presence of the acetylide bridge in **2** (Table 1),[15] while the presence of the diimine moiety is indicated by new infrared absorptions near 1594 and 1570 cm^{-1} attributable to the $C{=}N_{Imine}$ stretch and

(9) Le Stang, S.; Paul, F.; Lapinte, C. *Inorg. Chim. Acta* **1999**, *291*, 403−425.
(10) Paul, F. Unpublished results.
(11) Ibn Ghazala, S.; Paul, F.; Toupet, L.; Lapinte, C. *J. Organomet. Chem.* **2006**.
(12) Denis, R.; Toupet, L.; Paul, F.; Lapinte, C. *Organometallics* **2000**, *19*, 4240−4251.
(13) Goswami, S.; Kharmawphlang, W.; Deb, A. K.; Peng, S.-M. *Polyhedron* **1996**, *15*, 3635−3641.
(14) (a) Ruben, M. G.; Armando, A.-C. *J. Mol. Struct.* **2003**, *655*, 375−389. (b) Bianchini, C.; Lee, H. M.; Mantovani, G.; Meli, A.; Oberhauser, W. *New J. Chem.* **2002**, *26*, 387−397.
(15) Paul, F.; Mevellec, J.-Y.; Lapinte, C. *Dalton Trans.* **2002**, 1783−1790.

Table 1. Infrared Data for Selected Complexes in CH_2Cl_2 Solution[a] (cm^{-1})

compd[b]	$\nu_{C\equiv C}$ Fe(II)	$\nu_{C\equiv C}$ Fe(III)[c]	$\Delta\nu_{C\equiv C}$[d]	ref
[Fe]C≡C-4-$C_6H_4NH_2$ (**5**)	2056	1953	−103	15
[Fe]C≡C-4-C_6H_4N=CHPy (**2**)	2045	1960	−85	this work
[Fe]C≡C-4-C_6H_4N=CH-2-PyCu(PPh_3)Cl (**8**)	2035	1979	−56	this work
[{[Fe]C≡C-4-C_6H_4N=CH-2-Py}$_2$Cu][PF_6] (**9**[PF_6])	2029	1944	−85	this work

[a] Solid-state $\nu_{C\equiv C}$ values obtained in KBr pellets. [b] [Fe] ≡ (η^2-dppe)(η^5-C_5Me_5)Fe. [c] After in situ oxidation with excess ferrocenium hexafluorophosphate: only the main peaks were considered. [d] Neutral vs oxidized $\nu_{C\equiv C}$ difference.

Table 2. Electrochemical Data for Selected Complexes

compd[a]	$E_{1/2}$ (V)[b]	ΔE_p (V)	i_c/i_a	ref
[Fe]C≡C-4-$C_6H_4NH_2$ (**3**)	−0.25	0.08	1	12
[Fe]C≡C-4-C_6H_4N=CH-2-Py (**2**)	−0.16	0.08	1	this work
[Fe]C≡C-4-C_6H_4N=CH-2-PyCu(PPh_3)Cl (**8**)	−0.12	0.09	1	this work
[{[Fe]C≡C-4-C_6H_4N=CH-2-Py}$_2$Cu][PF_6] (**9**[PF_6])	−0.09	0.09	1	this work

[a] [Fe] ≡ (η^2-dppe)(η^5-C_5Me_5)Fe. [b] All *E* values in V vs SCE. Conditions: CH_2Cl_2 solvent, 0.1 M [N(^{n}Bu)][PF_6] supporting electrolyte, 20 °C, Pt electrode, sweep rate 0.100 V s^{-1}. The ferrocene/ferrocenium (Fc/Fc^+) complex was used as an internal reference for potential measurements ($E_{1/2}$ = 0.46 V).[17]

Table 3. UV−vis Data for Selected Fe(II) Complexes in CH_2Cl_2

compd[a]	abs (nm) ($10^{-3}\epsilon$ (M^{-1} cm^{-1}))
C_6H_5-N=CHPy (**7**)	280 (16.9); 314 (sh, 10.3)
[Fe]C≡C-4-$C_6H_4NH_2$ (**5**)	322 (17.6)
[Fe]C≡C-4-C_6H_4N=CHPy (**2**)	318 (19.7); 504 (14.4)
2$^+$	502 (7.8); 720 (4.7)
[Fe]C≡C-4-C_6H_4N=CH-2-PyCu(PPh_3)Cl (**8**)	342 (sh, 17.2); 606 (10.2)
8$^+$	372 (13.9); 512 (sh, 3.7); 708 (3.3)
[{[Fe]C≡C-4-C_6H_4N=CH-2-Py}$_2$Cu][PF_6] (**9**[PF_6])	366 (30.8); 522 (14.4); 704 (19.2)
9$^+$	376 (37.2); 512 (14.0); 710 (14.7)
9^{2+}	386 (39.4); 502 (sh, 16.2); 710 (6.6)

[a] [Fe] ≡ (η^2-dppe)(η^5-C_5Me_5)Fe.

to the C=N_{Py} stretch, respectively.[13,16] In comparison to the starting amino complex **5**, the $\nu_{C\equiv C}$ stretch has been shifted from ca. 15 cm^{-1} to lower energies.[15] The characteristic singlet corresponding to the primary carbon atom of the diimine ligand was also identified in the ^{13}C NMR spectra near 157 ppm with the help of HMQC correlations ($^1J_{CH}$ = 163 Hz).

Cyclic voltammetry performed on **2** reveals a reversible wave corresponding to the Fe(II)/Fe(III) oxidation at 0.16 V vs SCE, which also shows that the Fe(III) congener is stable at the electrode (Table 2 and Supporting Information). The UV−visible spectrum of this new Fe(II) complex was also recorded (Table 3) and shows a broad absorption near 500 nm (Figure 2). This electronic transition is at the origin of the garnet red color of the compound in solution and can be attributed to the MLCT transition usually observed for these acetylide complexes. Indeed, $\pi \rightarrow \pi^*$ or n $\rightarrow \pi^*$ transitions for an organic *N*-aryl-(2-pyridyl)2-aldimine such as the phenyl derivative **7** appear usually at wavelengths below 350 nm (Table 2).[16]

Reaction of the New "Organoiron" Ligand 2 with Cu(I) Complexes. In order to assess the capability of this new organometallic ligand to complex metal centers, we reacted it with Cu(I) precursors well-known to form complexes with diimine ligands. Thus, **2** was reacted in boiling acetonitrile with the copper(I) chloride polymer in presence of triphenylphosphine (Scheme 3a) and the new blue complex [(η^2-dppe)(η^5-C_5Me_5)-FeC≡C-4-C_6H_4N=CH-2-Py]Cu(PPh_3)Cl (**8**) was isolated in 70% yield.[18] This compound was characterized by mass spectrometry and by ^1H and ^{31}P NMR. In FAB-MS, a molecular ion corresponding to the complex after loss of a chloride ligand is clearly detected. The single peak observed near 101.4 ppm in ^{31}P NMR shows that a single compound containing our ligand has been isolated. An additional singlet of half intensity, which presumably corresponds to the coordinated triphenylphosphine in **8,** is also detected near −4.0 ppm.[19] These data were also corroborated by the corresponding ^1H NMR spectrum, which exhibited the expected signals for **8** with the right intensities. In addition, the infrared spectrum evidences the characteristic $\nu_{C\equiv C}$ stretch of the coordinated ligand **2** at 2035 cm^{-1} (Table 1) and again several peaks in the 1590 cm^{-1} region ($\nu_{C=N}$ stretches). Notably, concerning the $\nu_{C\equiv C}$ stretch in **8**, a 10 cm^{-1} shift to lower energy in comparison to **2** is apparent for the $\nu_{C\equiv C}$ stretch, which reveals that a decrease in the acetylide bond order occurred upon complexation of **2**. Cyclic voltammetry of **8** shows a reversible wave corresponding to the Fe(II)/Fe(III) oxidation at ca. −0.12 V vs SCE: i.e., at potentials slightly more positive than for **2** (Table 2 and the Supporting Information). The UV−vis spectrum obtained for **8** shows a spectrum resembling that of **2**, but both absorptions have been bathochromically shifted (Table 3 and Figure 2).

The reaction of **2** with the acetonitrile-solvated Cu(I) hexafluorophosphate salt in methanol gave also a new Cu(I) complex, **9**[PF_6], containing two coordinated diimine ligands (Scheme 3b). Blue crystals of this compound could be obtained by slow diffusion of *n*-pentane into a dichloromethane solution of the complex, and its solid-state structure (Figure 3), as well as some high-resolution FAB-MS measurements, confirmed the proposed

(16) Montalvo-Gonzales, R.; Ariza-Castolo, A. *J. Mol. Struct.* **2003**, *655*, 375−389.

(17) Connelly, N. G.; Geiger, W. E. *Chem. Rev.* **1996**, *96*, 877−910.

(18) Barron, P. F.; Engelhardt, L. M.; Healy, P. C.; Kildea, J. D.; White, A. H. *Inorg. Chem.* **1988**, *27*, 1829−1834.

(19) This ^{31}P NMR signal does not exhibit any coupling to the ^{63}Cu and ^{65}Cu isotopes of spin $^3/_2$ and comes out close to the shift of free triphenylphosphine. Given that no additional peak can be detected for **8** in this spectral range where the signal of the triphenylphosphine coordinated to Cu(I) is expected to appear,[18] most likely quadrupolar relaxation precludes the resolution of the coupling of ^{31}P to $^{3/2}Cu$ isotopes.[20]

(20) Berners-Price, S. J.; Johnson, R. K.; Mirabelli, C. K.; Faucette, L. F.; Mc Cabe, F. L.; Sadler, P. J. *Inorg. Chem.* **1987**, *26*, 3383−3387.

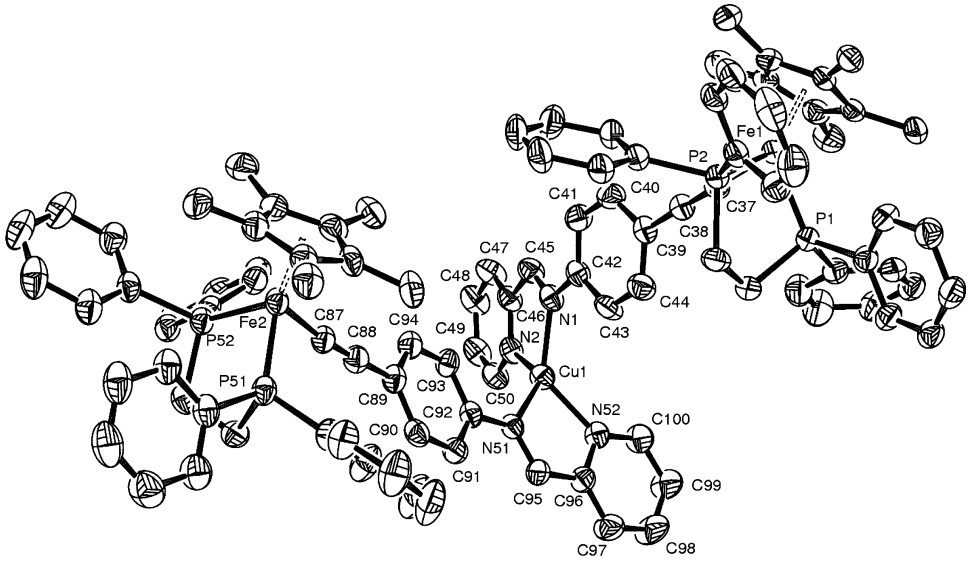

Figure 3. ORTEP representation of the bis-diimine copper complex **9**[PF_6] at the 50% probability level.

Scheme 3

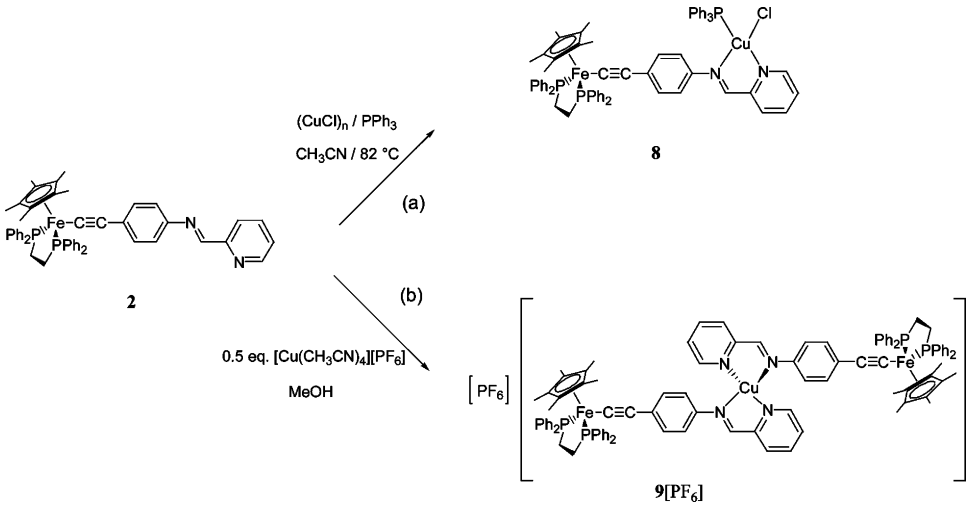

stoichiometry. The ^{31}P NMR spectrum exhibits a single peak at 100.9 ppm along with the characteristic quintet of the PF_6^- counterion around 143 ppm, and the corresponding ^1H NMR confirms the sole presence of the imine ligand **2** in the product. We noticed that the resolution of the ^1H NMR spectrum of **9**[PF_6] was poorer than that obtained for **8**. This phenomenon cannot be attributed to adventitious traces of oxidized material, since the dppe singlet on the ^{31}P NMR spectrum should not have been so sharp ($\Delta\nu_{1/2} \leq 10$ Hz) in the case of self-exchange.[21] We then recorded the ^1H and ^{31}P NMR spectra of **9**[PF_6] at lower temperatures and showed that the complex was fluxional in solution at ambient temperature, since the ^1H and ^{31}P NMR signals broaden and give rise to two sets of signals at 198 K (see the Supporting Information). This phenomenon, which presents an activation enthalpy around 46 kJ mol^{-1}, is certainly responsible for the unusual line broadening observed at ambient temperature with **9**[PF_6].[22] The infrared spectrum of **9**[PF_6] is also diagnostic of the coordination of the metallo ligand **2**. It shows a ca. 15 cm^{-1} shift to lower energy of the characteristic $\nu_{C\equiv C}$ stretch in comparison to that of the free ligand **2** (Table 1), both in the solid state and in solution. The observation of a shoulder on the $\nu_{C\equiv C}$ stretch of the two functional diimine ligands in **9**[PF_6] at 1995 cm^{-1} and also the presence of two medium peaks at 1587 and 1572 cm^{-1} can be traced back to the existence of isomers, as evidenced by NMR. Alternatively, the shoulders on the $\nu_{C\equiv C}$ stretch could have also originated from vibronic coupling between equivalent vibrators in **9**[PF_6]. We therefore logically wondered about the electronic interaction between the organoiron redox-active centers in the mixed-valent (MV) state of this compound. In this connection, cyclic voltammetry of **9**[PF_6] reveals only a single reversible wave (Supporting Information) corresponding to the oxidation of both Fe(II) centers at a potential slightly more positive (ca. 0.09 V vs SCE) than those previously observed for **8** and **2** (Table 2). The peak-to-peak separation of this signal is only marginally larger than that recorded for **2**, suggesting that the two Fe(III/II) oxidation potentials are very close. Thus, the electronic communication between the two equivalent redox centers in **9**[PF_6], if any, is not apparent on the cyclic voltammograms. According to our voltammogram (Supporting Information), the Cu(I)/Cu(II) oxidation **9**[PF_6] must occur

(21) Paul, F.; da Costa, G.; Bondon, A.; Gauthier, N.; Sinbandhit, S.; Toupet, L.; Costuas, K.; Halet, J.-F.; Lapinte, C. *Organometallics* **2007**, *26*, 874.

(22) On the basis of the X-ray structure of **9**[PF_6], we would tentatively suggest that we have a rapid interconversion between two isomers presenting the Cu(I) center in a distorted-tetrahedral coordination sphere with the organoiron groups in distal and proximal positions.

Table 4. Crystal Data, Data Collection, and Refinement Parameters for 2 and 9[PF_6]

	2·$^1/_4CH_2Cl_2$	**9**[PF_6]·$^3/_2CH_2Cl_2$
formula	$FeP_2C_{50}H_{48}N_2$·0.25CH_2Cl_2	$Fe_2CuP_4C_{100}H_{96}N_4$-$PF_6C_5H_{12}$·0.5$C_5H_{12}$
fw	816.43	1888.08
temp (K)	150(1)	120(1)
cryst syst	monoclinic	monoclinic
space group	*C*2/*c*	$P2_1/n$
a (Å)	21.3913(3)	21.3702(5)
b (Å)	12.0035(2)	18.4998(4)
c (Å)	33.2222(4)	27.0213(6)
α (deg)	90.00	90.00
β (deg)	90.258(1)	103.391(1)
γ (deg)	90.00	90.00
V (Å^3)	8530.4(2)	10392.3(4)
Z	8	4
D_{calcd} (g cm^{-3})	1.271	1.207
cryst size (mm)	0.35 × 0.35 × 0.80	0.38 × 0.15 × 0.08
F(000)	3428	3946
diffractometer	KappaCCD (Nonius)	KappaCCD (Nonius)
abs coeff (mm^{-1})	0.497	0.667
data collecn		
θ_{max} (deg)	27.5	27.5
no. of frames	374	290,
ω rotation (deg)	1.0	2.0
s/frame	10	180
θ range (deg)	2.67−25.36	1.90−27.12
hkl range	0−25, 0−14,-−39 to +40	0−27, 0−23,-−34 to +33
total no. of rflns	34 608	85 601
no. of unique rflns	7798	22 884
no. of obsd rflns ($I > 2\sigma(I)$)	6255	13862
no. of restraints/params	0/510	0/1153
a, *b*[a]	0.0911, 28.9131	0.1144, 18.2658
final *R*	0.055	0.077
R_w	0.155	0.184
R (all data)	0.073	0.150
R_w (all data)	0.169	0.234
goodness of fit (F^2) (S_w)	0.995	1.008
$\Delta\rho_{max}$ (e Å^{-3})	1.082	0.665
$\Delta\rho_{min}$ (e Å^{-3})	-0.512	-0.811

[a] $w = 1/[\sigma^2(F_o)^2 + (aP)^2 + bP]$ (where $P = [F_o^2 + F_c^2]$).

above 1 V vs SCE in dichloromethane.[23] The UV−visible spectrum of this new complex was also recorded and shows an additional transition (Table 3 and Figure 2). Thus, a broad absorption is observed near 700 nm at the origin of the dark blue color of the complex, and a second transition near 512 nm is also present in the visible range.

Solid-State Structures of 2 and 9[PF_6]. Both compounds crystallize in monoclinic space groups with solvate molecules in the cell (Table 4, Figures 1 and 3). In the solid-state structure of the organometallic diimine compound **2**, two molecules are arranged in a kind of centrosymmetric dimeric unit. For the complex **9**[PF_6], the molecules prefer to stack along an intramolecular axis joining the copper atom and the point bisecting the Fe−Fe axis, although no strong intermolecular interactions are apparent from the atomic distances. These spatial arrangements are certainly adopted to minimize the voids within the cells.

Regarding the diimine moiety in **2**, the N−N′ trans conformation is like that obtained for the *trans*-*N*-(2-pyridylmethylene)aniline. The dihedral angle (*β* = C41−C42−N1−C45) between the phenyl plane of the aniline ring and that of the diimine site is larger in **2**, however (28.8° vs 17.9/8.9°).[24] Such an angle is due to steric repulsions between the ortho hydrogen atom of the aniline ring and the hydrogen atoms bonded to the methyne carbon.[16] In **2**, the diimine site adopts a rather perfectly planar trans arrangement for the diimine site, as shown by the corresponding dihedral angle of 0.2° (α = N1−C45−C46−N2). Note that, once complexed, the diimine unit in **9**[PF_6] is slightly less planar (α = 1.8°) and also shows a diminished *β* angle (12.5°), in line with an improved *π* conjugation over the whole *N*-phenyl(2-pyridyl)aldimine core.

Concerning the organoiron end groups of the molecules, the bond distances and angles are as usually found for these pianostool Fe(II) arylacetylide moieties (Table 5).[12,25,26] As discussed

Table 5. Selected Bond Lengths (Å) and Angles (deg) for 2 and 9[PF_6]

	2·$^1/_4CH_2Cl_2$	**9**[PF_6]·$^3/_2CH_2Cl_2$
Bond Lengths		
Fe1−Cp*(centroid)[a]	1.735	1.735
Fe2−Cp*(centroid)		1.733
Fe1−P1	2.1746(9)	2.1653(13)
Fe1−P2	2.1941(9)	2.1795(14)
Fe1−C37	1.893(3)	1.882(5)
C37−C38	1.221(4)	1.227(7)
C38−C39	1.434(4)	1.407(7)
C42−N1	1.416(4)	1.407(6)
N1−C45	1.259(5)	1.287(6)
C45−C46	1.471(5)	1.458(7)
Fe2−P51		2.1791(15)
Fe2−P52		2.1772(14)
Fe2−C87		1.881(5)
C87−C88		1.225(7)
C88−C89		1.435(7)
C92−N51		1.424(6)
N51−C95		1.295(6)
C95−C96		1.450(6)
Cu−N1		2.024(4)
Cu−N2		2.013(4)
Cu−N51		2.033(4)
Cu−N52		2.023(4)
Fe1−Cu1		9.98
Fe2−Cu1		9.98
Fe1−Fe2		11.89
Bond Angles		
P1−Fe1−P2	86.50(3)	85.31(5)
P1−Fe1−C37	82.50(10)	84.11 (15)
P2−Fe1−C37	86.72(10)	87.22(15)
Fe1−C37−C38	178.8(3)	176.8(4)
C42−N1−C45	119.1(3)	121.7(4)
P51−Fe2−P52		86.13 (5)
P51−Fe2−C87		85.00(16)
P52−Fe2−C87		87.96(15)
Fe2−C87−C88		174.0(4)
C92−N1−C95		120.3(4)
N1−Cu1−N2		81.77(17)
N1−Cu1−N51		120.79(16)
N51−Cu1−N52		81.32(16)
Dihedral Angles		
Fe1−Cp*(centroid)/C39−C40	77.3	35.5
Fe2−Cp*(centroid)/C89−C90		121.8
C41−C42/N1−C45	7.6	9.9
C91−C92/N51−C95		0.2
N1−C45/C46−N2	0.2	1.8
N51−C95/C96−N52		7.6
N1−N2/N51−N52		101.2

[a] Cp* = pentamethylcyclopentadienyl ligand.

(23) The Cu(I)/Cu(II) oxidation potential had been previously reported to occur around 0.35 V vs SCE in methanol for the related homoleptic Cu(I) complex with the *N*-phenyl(2-pyridyl)aldimine ligand.[13] This oxidation is apparently quite solvent sensitive, since we have presently verified that the same complex is oxidized irreversibly around 0.9 V vs SCE in dichloromethane (Supporting Information) and gives rise to electrodeposition of unknown materials on the electrode.

(24) Wiebcke, M.; Mootz, D. *Acta Crystallogr., Sect. B* **1982**, *38*, 2008−2013.

(25) Costuas, K.; Paul, F.; Toupet, L.; Halet, J.-F.; Lapinte, C. *Organometallics* **2004**, *23*, 2053−2068.

(26) Paul, F.; Toupet, L.; Thépot, J.-Y.; Costuas, K.; Halet, J.-F.; Lapinte, C. *Organometallics* **2005**, *24*, 5464−5478.

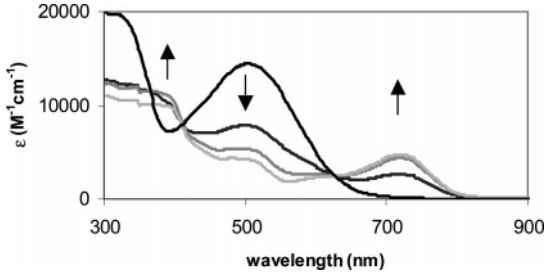

Figure 4. Spectroelectrochemical monitoring of the oxidation of **2**.

above, the diimine fragment is more coplanar than the C═N−aryl moiety in both compounds, suggesting a stronger π conjugation between π bonds in the former fragment. Otherwise, bond lengths for the C−C(═N) group in the free imine fragment in **2** or after complexation in **9**[PF_6] are also as usual.[27] Thus, the geometry around the Cu(I) center in **9**[PF_6] compares quite well with that previously observed in related complexes by Goswami et al.[13] Likewise, the Cu−N distances are slightly shorter in the case of the pyridine nitrogen atoms relative to the diimine ones, in line with previous observations.[13] Finally, one can notice a slight deviation from strict tetrahedral geometry, the angle between the mean planes defined by the diimine ligands being closer to 75° than to 90°, a distortion likely attributable to the steric interaction with the bulky organoiron substituents of neighboring molecules. Apparently, the two piano-stool fragments in $\mathbf{9}^+$ are somewhat puckered by these intermolecular contacts, since the deviation from strict linearity of the Fe−acetylide axis is somewhat more pronounced in **9**[PF_6] than in **2**. However, the bond lengths within these fragments are not significantly perturbed. The intramolecular Fe−Fe distance is 11.89 Å, while both Fe(II) atoms are equidistant (9.97 Å) from the copper center. Actually, the shortest metal−metal contacts are intermolecular in **9**[PF_6], being 8.60 Å for Fe−Fe distances and 7.72 Å for Fe−Cu distances.

Brief Characterization of the Oxidized States of 2, 8, and 9[PF_6] by Spectoelectrochemistry and ESR. Given the chemically reversible nature of the voltammograms obtained for **2**, **8**, and **9**[PF_6], we wondered about the stability of the corresponding oxidized states and about the electronic properties of these compounds. Also, an important question was whether or not a weak electronic coupling exists between the two iron centers in the mixed-valent (MV) compound $\mathbf{9}^{2+}$.

In order to answer these questions, we first generated the radical cation of the metallo ligand **2**[PF_6] in a spectroelectrochemical cell and observed its electronic absorptions. Upon oxidation, the low-energy band diminished and another less intense band appeared at ca. 720 nm (Table 3 and Figure 4). The presence of isosbestic points suggests that only one new species was generated in solution upon oxidation. Thus, **2**[PF_6] is cleanly generated and seems quite stable in solution, as the oxidation proved quasi-reversible (loss of less than 10% based on UV intensity after 2.5 h in solution). Then, using a more concentrated solution and generating **2**[PF_6] in situ with ferrocenium hexafluorophosphate, a very weak LF transition could be detected in the near-IR range, near 1830 ± 10 nm (Figure 5b). Finally, the infrared spectrum obtained for the oxidized product after evaporation of the solvent revealed a shift of ca. 95 cm^{-1} toward the lower wavenumbers of the diagnostic $\nu_{C\equiv C}$ stretch, which appeared now at 1960 cm^{-1} (Table 1), with a shoulder at 1997 cm^{-1}. The $\nu_{C=N}$ stretches were also shifted, but comparatively much less.

We next performed similar experiments on the neutral copper complex **8**. Again a very similar behavior could be observed in the spectroelectrochemical cell, consisting of a hypsochromic shift of the intense low-energy band along with the appearance of a new band in the 700 nm spectral region (Table 3). Note that the maxima observed for the oxidized complex **8**[PF_6] were slightly shifted relative to these of **2**[PF_6], in line with the coordinated nature of the metallo ligand in **8**[PF_6]. Also, after in situ chemical oxidation with ferrocenium hexafluorophosphate using a more concentrated solution, we could detect a broad and weak ($\epsilon = 140 \pm 20$ M^{-1} cm^{-1}) absorption near 1870 ± 10 nm (Figure 5a). The infrared spectra of the solid obtained after evaporation of this solution revealed a broad $\nu_{C\equiv C}$ stretch centered at ca. 1978 cm^{-1} (Table 1). Many shoulders are apparent on this very weak absorption at 2034, 1998, 1898, and 1948 cm^{-1}.

Finally, the spectroelectrochemical oxidation of **9**[PF_6] was effected (Figure 6). Upon oxidation, the very intense band of **9**[PF_6] at 704 nm decreased in energy and a new band appeared around 710 nm, while the weaker band at ca. 522 nm slightly shifted to 502 nm. The final spectrum observed for $\mathbf{9}^{3+}$ is reminiscent of that observed for **2**[PF_6]. Note that, in this case, the oxidation was not reversible; this fact might be related to the deposition of some material on the electrochemical grid in the cell. Also, a new broad and weak absorption near 1830 ± 10 nm ($\epsilon = 205 \pm 20$ M^{-1} cm^{-1}) could be detected in the near-IR range from freshly prepared solutions of **9**[PF_6] containing 1 and 2 equiv of ferrocenium hexafluorophosphate (Figure 5a). Also, the infrared spectra of the solid obtained after evaporation of these solutions revealed the progressive conversion of the starting compound **9**[PF_6] into a compound featuring a single $\nu_{C\equiv C}$ stretch at ca. 1944 cm^{-1} (Table 1) with a shoulder at 2003 cm^{-1}. Note that in none of these experiments was a specific set of absorptions observed when roughly half of the starting complex **9**[PF_6] had been oxidized: i.e., corresponding to the situation where the mixed-valent complex $\mathbf{9}^{2+}$ should have been prevalent in the reaction mixtures.

In order to gain further insight into the properties of these oxidized species, we have recorded their ESR spectra in solvent glasses at 80 K, after performing the oxidation in situ using ferrocenium hexafluorophosphate. For **2**[PF_6], the typical rhombic signature of a metal-centered radical was observed (Table 6 and Figure 7). The corresponding radical cation **8**[PF_6] was also generated with the ferrocenium hexafluorophosphate salt in the same solvent glass at 80 K, and its ESR spectrum was recorded. A rhombic signature was again found with a slightly improved anisotropy. Another radical was also detected in small amounts corresponding to a very broad isotropic signal at $g_{iso} \approx 2.13$ ($\Delta H_{pp} \geq 180$ G). It is tentatively attributed to a side reaction of $\mathbf{8}^+$ occurring in the ESR matrix. Finally, after we had checked that **9**[PF_6] was ESR-silent, the spectra of its mono- and dioxidized parents were recorded at 80 K. Only in the first case was a clean rhombic signal obtained with an anisotropy also slightly larger than that of the free ligand (Figure 7). This signal most probably corresponds to the MV complex $\mathbf{9}^{2+}$. With regard to **9**[PF_6]$_3$, a much poorer and less intense spectrum was obtained (Supporting Information). Apparently, only a rhombic signal resembling that of $\mathbf{2}^+$ is detected, while a broad and isotropic signal would have been expected for the putative $\mathbf{9}^{3+}$ species.[28] Most likely, the latter is presently not

(27) Allen, F. H.; Kennard, O.; Watson, D. G.; Brammer, L.; Orpen, A. G.; Taylor, R. *J. Chem. Soc., Perkin Trans. 2* **1987**, S1−S19.

(28) Weyland, T.; Costuas, K.; Toupet, L.; Halet, J.-F.; Lapinte, C. *Organometallics* **2000**, *19*, 4228−4239.

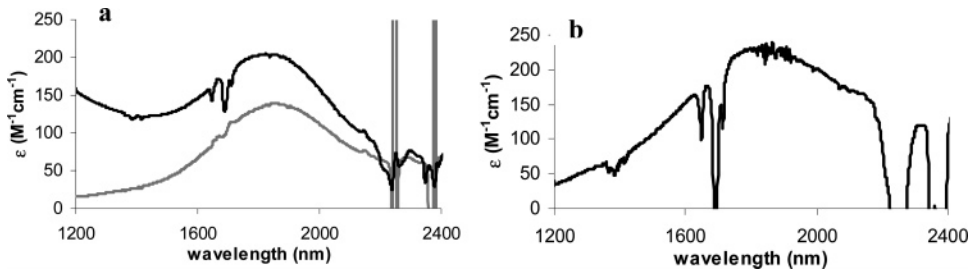

Figure 5. (a) LF absorption in the near-IR range for isolated samples of complexes $\mathbf{8}^{+}$ and $\mathbf{9}^{3+}$. (b) LF absorption for $\mathbf{2}^{+}$ observed during spectroelectrochemical investigations.

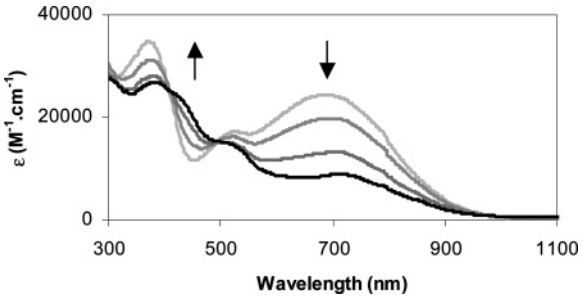

Figure 6. Spectroelectrochemical monitoring of the oxidation of $\mathbf{9}[PF_6]$.

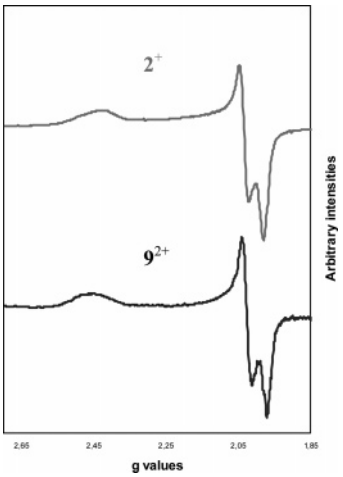

Figure 7. ESR spectra of $\mathbf{2}[PF_6]$ (gray trace) and $\mathbf{9}[PF_6]_2$ (black trace) in 1,2-DCE/DCM glasses at 70 and 80 K, respectively.

Table 6. ESR Spectroscopic Data for $[(\eta^2\text{-dppe})(\eta^5\text{-}C_5Me_5)FeC{\equiv}CAr][PF_6]$ Complexes

compd	Δg	g_1	g_2	g_3	$\langle g \rangle$
$\mathbf{2}^{+}$	0.447	2.428	2.034	1.981	2.147
$\mathbf{8}^{+}$	0.482	2.460	2.033	1.978	2.157
$\mathbf{9}^{2+}$	0.49	2.46	2.03	1.97	2.15

detected, owing to the fast electronic relaxation experienced by such diradicals.

Discussion

First of all, the experimental data available for **2** suggest that, in this compound, the *p*-diimine substituent is clearly less electron-releasing than the amino group. Thus, the metal-centered oxidation occurs at significantly lower potential than for the starting amino complex **3** and actually comes quite close to that of a complex with a tolyl group such as **10** (Chart 2), suggesting that the *p*-2-aldimine group resembles a methyl substituent in terms of global substituent effect (as given by the regular σ substituent parameters[29]).[25]

Chart 2

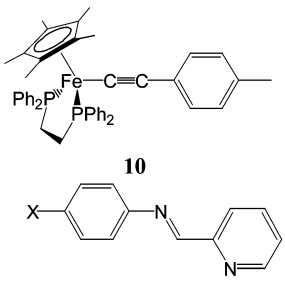

11a-c (X = Cl, H, CH_3)

Scheme 4

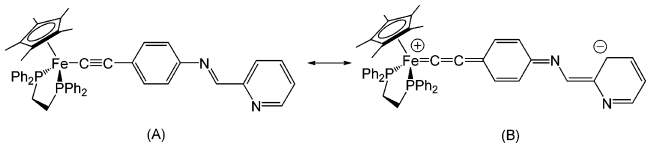

Then, on the basis of the electronic (MLCT) transition observed for **2** (near 500 nm), which appears at energy significantly lower than that recorded for **10** (at 339 nm), or on the basis of the $\nu_{C\equiv C}$ band at 2045 cm^{-1} of **2**, which also lies below that of **10** (2060 cm^{-1}),[15,25] it seems that the (2-pyridyl)-aldimine substituent in **2** resembles a cyano group in terms of mesomeric properties (as given by the σ^{-} parameter[29]).[25]

Alternatively, using the LFER (eqs 1a,b, $R = 0.998$) previously proposed by Jovanovic et al. for para-substituted *N*-aryl(2-pyridine)aldimines such as **11a**−**c** (Chart 2), the electronic substituent parameter for the "$(\eta^2$-dppe$)(\eta^5$-$C_5Me_5)$-FeC≡C−" fragment can be deduced from the ^{13}C NMR shift of the methine carbon.[30] According to eq 1b, this fragment

$$\Delta\delta_C = \delta_C{}^X - \delta_C{}^H \quad (1a)$$

$$\Delta\delta_C = 3.20\sigma_p{}^+ + 0.24 \quad (1b)$$

would correspond to a σ^{+} electronic substituent parameter (ESP) of ca. −0.99, which is comparable to that of a methoxy group ($\sigma_p{}^+ = -0.78$).[7] This value is perfectly in line with a previous estimate of the electron-releasing capability of this fragment. Thus, as shown in Scheme 4, it seems that the valence bond (VB) structure (B) will present a non-negligible weight in the ground state (GS) VB description of **2**.

We have then shown that **2** can coordinate to Cu(I) centers and gives a fluxional complex in the case of $\mathbf{9}[PF_6]$. Upon complexation, a red shift of the low-energy absorption is at the origin of the color change from red to dark blue (Figure 2).

(29) Hansch, C.; Leo, A.; Taft, R. W. *Chem. Rev.* **1991**, *91*, 165−195.
(30) Jovanovic, B. Z.; Misic-Vukovic, M.; Marinkovic, A. D.; Vajs, V. *J. Mol. Struct.* **2002**, *642*, 113−118.

While this absorption corresponds to a $d_{Fe} \rightarrow \pi_{C\equiv C}^*$ MLCT transition in **2**,[25] its attribution a priori is more problematic for the complexes **8** and **9**[PF_6], which contain the Cu(I) center and are also relatively electron-rich. Goswami and co-workers have previously studied a series of Cu(I) complexes similar to **9**[PF_6] with the organic *N*-aryl(2-pyridyl)aldimines **11a**−**c**.[13] These researchers reported an intense ($\epsilon \approx 2.4 \times 10^3\ M^{-1}\ cm^{-1}$) $d_{Cu} \rightarrow \pi_{C=N}^*$ MLCT transition in the visible range (485−495 nm) for these compounds, which is shifted to higher wavelengths when the aryl substituent becomes more electron-releasing. Thus, the low-energy transition detected at ca. 700 nm in **9**[PF_6] can be associated with the $d_{Fe} \rightarrow \pi_{C\equiv C}^*$ MLCT transition of **2** bathochromically shifted by coordination of the cationic Cu(I) center to the (2-pyridyl)aldimine site, while the transition at 522 nm certainly corresponds to the $d_{Cu} \rightarrow \pi_{C=N}^*$ MLCT transition in **9**[PF_6], shifted to higher wavelengths due to the presence of the strongly electron releasing "Cp*(dppe)Fe−C≡C−" fragment appended to the N-aryl group of the coordinated (2-pyridyl)aldimine ligand. In **8**, only the $d_{Fe} \rightarrow \pi_{C\equiv C}^*$ MLCT transition is observed. Possibly, the less intense $d_{Cu} \rightarrow \pi_{C=N}^*$ MLCT transition, if any, is burried within the broad MLCT absorption. Unsurprisingly, the $d_{Fe} \rightarrow \pi_{C\equiv C}^*$ MLCT is less shifted than in **9**[PF_6] due to the neutral nature of the complex **8**, rendering the Cu(I) less π-acidic than in **9**[PF_6], in line with the lesser effect of **8** relative to that of **9**[PF_6] on the Fe(II)/Fe(III) oxidation potential (Table 2) and on the $\nu_{C\equiv C}$ stretch (Table 1). In accordance with these data, an increasing weight of the valence bond (VB) form B (Scheme 4), in the order **2** < **8** < **9**[PF_6], can be inferred from the GS of these compounds. On the basis of LFERs previously established for this class of Fe(II) acetylide complexes,[25] this increase might be attributed to the improved electron-withdrawing capability of the (2-pyridyl)aldimine fragment in **2,** on complexation to increasingly Lewis acidic metal centers. Qualitatively similar changes induced by coordination have previously been reported for **1a**,**b**.[9]

We have also briefly examined the oxidized states of these compounds. In line with previous investigations on related Fe(III) complexes,[15,25,26] **2**[PF_6] exhibits the expected spectroscopic signatures for a metal-centered Fe(III) radical cation and appears fairly stable in solution. Thus, the imine-centered MLCT in **2** shifts to higher energy upon oxidation and a new band near 800 nm grows, which most probably corresponds to a $\pi \rightarrow d_{Fe}$ LMCT band.[26] The rather low value found for the anisotropy (ca. 0.44) is comparable to that of the 4-tolylalkynyl Fe(III) radical **10**$^+$ and suggests that some delocalization of the unpaired electron takes place on the functional arylacetylide ligand. Also, upon oxidation, infrared spectroscopy reveals that the acetylide bond is weakened, due to the delocalization of the unpaired electron, as usually observed with such compounds.[26,31]

Once complexed to the "(Ph_3P)ClCu" moiety, this metallo ligand can still be oxidized and gives also rise to fairly stable radical species such as **8**[PF_6]. The spectroscopic signatures of **8**[PF_6] strongly resemble those of **2**[PF_6]. For instance, the former also exhibits a LF transition very close in energy in the near-IR range and presents a quite similar anisotropy for its rhombic ESR signal. Actually, on the basis of the anisotropy values, the unpaired electron might be a little less delocalized on the acetylide ligand in **8**[PF_6] than in **2**[PF_6]. Thus, the complexation of the (2-pyridyl)aldimine site of **2** to the Cu(I) center has increased the electron-withdrawing power of the (2-pyridyl)aldimine moiety, which translates into an improved localization of the unpaired electron on the iron center after oxidation. In line with this statement, no hyperfine coupling to the copper can be detected,[32] evidencing that the unpaired electron only marginally resides on the Cu center in **8**[PF_6].

Similarly, two oxidized states might be generated from **9**[PF_6], which presents two coordinated (2-pyridyl)aldimine ligands, like **2**. Actually, after complete oxidation, the resulting electronic spectrum obtained for the fully oxidized **9**$^{3+}$ complex strongly resembles that obtained for the free ligand **2**$^+$. Also, the impossibility of reverting to the starting complex or of inducing any visible change on the spectra by reduction, after monitoring the oxidation during the spectroelectrochemical investigations with concentrated solutions (ca. 5×10^{-3} M), suggests that some oxidatively induced decomposition occurred and resulted in passivation of the working electrode. However, this decomposition process is apparently slow and not kinetically relevant when oxidation is performed more rapidly using adapted oxidants such as ferrocenium salts. Indeed, infrared spectra of freshly prepared samples of **9**[PF_6]$_2$ and **9**[PF_6]$_3$ reveal that the oxidized ligands most likely remain coordinated to the Cu(I) center in **9**[PF_6]$_2$ and **9**[PF_6]$_3$, since the spectral fingerprints of these complexes in the acetylide region differ from those of **2**[PF_6].

Then, there is a very important question with regard to whether or not any electron transfer occurs between the two redox-active Fe centers, either through space or through the central Cu(I) site, in the mixed-valent state **9**$^{2+}$. As suggested by ESR and infrared of in situ generated samples, the latter compound can be cleanly generated by chemical oxidation and seems fairly stable at room temperature (Tables 1 and 6). At 80 K, it exhibits a rhombic ESR signal with anisotropy slightly larger than that found for **2**[PF_6] and **8**[PF_6], but again, no hyperfine coupling to copper can be detected. The cyclic voltamogram has already shown that, if existent, the electronic coupling between the redox sites will be weak in **9**$^{2+}$, since no detectable splitting of the Fe(II/III) oxidations was observed. In this respect, the spectroelectrochemical study of **9**[PF_6] further confirms that the electronic coupling between the Fe(II/III) redox centers is negligible, since no electronic transition peculiar to the MV state nor any intervalence charge transfer (IVCT) band that could have corresponded to the Fe(III)/Fe(II) photoinduced electron transfer were detected. Also, on the infrared spectra, no $\nu_{C\equiv C}$ stretch particular to the MV state could be detected, further suggesting that each metallo ligand in **9**[PF_6] behaves independently from the other. On the basis of these results, the MV complex **9**[PF_6]$_2$ should therefore be categorized as a class I MV complex in the classification of Robin and Day.[33] Thus, given the very weak or nonexistent electronic coupling evidenced between the two organoiron redox-active end groups in **9**[PF_6]$_2$, the cationic Cu(I) center appears strongly insulating, like several Pt(II) centers previously studied.[9,34] However, instead of the square-planar geometries offered by Pt(II) sites, we have shown here that this insulating templating cation provides access to (pseudo) tetrahedral geometries, at least in the solid state.

Conclusion

We have reported the successful isolation and complete characterization of the new redox-active complex **2**, bearing a

(31) Paul, F.; Ellis, B. J.; Bruce, M. I.; Toupet, L.; Roisnel, T.; Costuas, K.; Halet, J.-F.; Lapinte, C. *Organometallics* **2006**, *25*, 649−665.

(32) Since it is not resolved in the ESR spectrum, the magnitude of the hyperfine coupling to copper must be less than 48/4 ≈ 12 G.

(33) Robin, M. B.; Day, P. *Adv. Inorg. Chem. Radiochem.* **1967**, 247−422.

(34) Richardson, G. N.; Vahrenkamp, H. *J. Organomet. Chem.* **2000**, *593*−*594*, 44−48.

(2-pyridyl)aldimine site at the para position on the aryl ring. We have also conclusively shown that this complex constitutes a metallo ligand, which opens a simple access to various polynuclear open-shell architectures using simple coordination reactions. Accordingly, **2** reacts with various Cu(I) precursors to give complexes similar to those formed with purely organic (2-pyridyl)aldimines. Due to the electron richness of the redox-active Fe(II) center in **2**, this metallo ligand allows for the in situ genesis of the corresponding oxidized polynuclear parents using mild oxidants. For instance, the closed-shell Fe(II)/Cu(I) and Fe(II)/Cu(I)/Fe(II) assemblies could be converted into the corresponding open-shell redox congeners Fe(III)/Cu(I) and Fe(III)/Cu(I)/Fe(III) with ferrocenium hexafluorophosphate. We have shown as well that, depending on the redox state of the iron in **2** and also depending on the coordination (or not) of a Lewis acidic center to the diimine site of **2**, specific changes in the electronic distribution occur within the iron alkynyl core. On the one hand, complexation increases the weight of the charge-delocalized VB form in the diimine moiety in closed-shell complexes (B, Scheme 4); on the other hand it enforces the localization of the unpaired electron on the iron center in the open-shell species. Allied to the intrinsic lability evidenced for **2** in **9**[PF_6], the latter effect proved detrimental to obtain a good electronic coupling between the two iron centers in the trinuclear MV Fe(III)/Cu(I)/Fe(II) complex $\mathbf{9}^{2+}$. As a result, a negligible electronic interaction between the organoiron units was evidenced in all redox states. More precisely, $\mathbf{9}^{2+}$ behaves as a class I MV complex in the classification of Robin and Day, evidencing that cationic Cu(I) metal centers behave as efficient insulators.

Experimental Section

General Data. All manipulations were carried out under inert atmospheres. Solvents and reagents were used as follows: Et_2O and *n*-pentane, distilled from Na/benzophenone; CH_2Cl_2, distilled from CaH_2 and purged with argon; $HN(^iPr)_2$, distilled from KOH and purged with argon; aryl bromides (Acros, >99%), opened/stored under Ar. The [(η^5-C_5H_5)$_2$Fe][PF_6] ferrocenium salt was prepared by previously published procedures.[17] Transmittance FT-IR spectra were recorded using a Bruker IFS28 spectrometer (400−4000 cm^{-1}). Raman spectra of the solid samples were obtained by diffuse scattering on the same apparatus and recorded in the 100−3300 cm^{-1} range (Stokes emission) with a laser excitation source at 1064 nm (25 mW) and a quartz separator with a FRA 106 detector. Near-IR spectra were recorded using a Bruker IFS28 spectrometer, using a Nernst Globar source and a KBr separator with a DTGS detector (400−7500 cm^{-1}) or tungsten source and a quartz separator with a Peltier-effect detector (5200−12 500 cm^{-1}) or on a Cary 5 spectrometer. UV−visible spectra were recorded on an UVIKON XL spectrometer. ESR spectra were recorded on a Bruker EMX-8/2.7 (X-band) spectrometer. MS analyses were performed at the "Centre Regional de Mesures Physiques de l'Ouest" (CRMPO, University of Rennes) on a high-resolution MS/MS ZABSpec TOF Micromass spectrometer. Elemental analyses were performed at the "Centre Regional de Mesures Physiques de l'Ouest" (CRMPO, University of Rennes).

Synthesis of (η^2-dppe)(η^5-C_5Me_5)Fe−C≡C-1,4-C_6H_4N=CH-2-Py (2). Method 1. In a Schlenk tube, to a mixture of 0.96 g (1.37 mmol) of (η^2-dppe)(η^5-C_5Me_5)Fe−C≡C-1,4-$C_6H_4NH_2$ (**5**) and 1 equiv of 2-pyridinecarboxaldehyde (**6**; 0.13 mL) was added 20 mL of methanol under argon. The purple reaction mixture was stirred for 24 h. The solvent was then removed under vacuum. The residue was subsequently washed with *n*-pentane and left under vacuum for a night at 50 °C to eventually provide 0.77 g (0.97 mmol) of the desired compound **2** as a dark orange powder. Yield: 71%. The compound can be crystallized by slow diffusion of *n*-pentane in a dichloromethane solution of **2**. Anal. Calcd for $C_{50}H_{48}N_2P_2Fe\cdot CH_2Cl_2$: C, 69.63; H, 5.73 N, 3.18. Found: C, 70.75; H, 5.86; N, 3.28. MS (FAB$^+$, *m*-NBA): *m*/*z* 794.264 ([M]$^+$, 100%); *m*/*z* calcd for [$C_{50}H_{48}N_2P_2Fe$] 794.264. FT-IR (KBr; ν_{max}/cm^{-1}): 2045 (s, C≡C), 1617 (w, C=N, imine), 1571 (m, C=N, Py and imine). $^{31}P\{^1H\}$ NMR (81 MHz, $CDCl_3$, H_3PO_4; δ_P): 101.4 (s, 2P, dppe). ^1H NMR (200 MHz, $CDCl_3$, Me_4Si; δ_H): 8.72 (d, 1H, J_{HH} = 3.9 Hz, H_6 Py); 8.64 (s, 1H, N=C*H*); 8.22 (d, 1H, J_{HH} = 7.9 Hz, H_3 Py); 7.84 (m, 2H, H_4 Py, H_5 Py); 7.38−6.81 (m, 22H, H_{aryl} and H_{dppe}); 6.83 (d, 2H, J_{HH} = 7.4 Hz, H_{aryl}); 5.33 (d, 2H, CH_2Cl_2); 2.69 (m, 2H, PCH_2); 2.01 (m, 2H, PCH_2); 1.45 (s, 15H, C_5Me_5). $^{13}C\{^1H\}$ NMR (125 MHz, $CDCl_3$, Me_4Si; δ_C): 157.3 (s, $^1J_{CH}$ = 163 Hz, *C*H=N); 155.1 (s, C_{Py}); 149.5 (s, *C*H$_{Py}$); 145.5 (s, *C*N=C); 136.5 (s, *C*H$_{Py}$); 138.4−134.2−127.1 (*C*H$_{Ar/dppe}$, Fe−*C*≡C and C≡C−*C*); 131.9 (s, *C*H$_{Ar}$); 124.5 (*C*H$_{Py}$); 121.7 (s, *C*H$_{Py}$); 120.8 (s, *C*H$_{Ar}$); 120.5 (s, Fe−C≡*C*); 87.1 (s, C_5Me_5); 30.1 (m, *C*H$_2$); 10.5 (s, C_5Me_5).

Method 2. In a Schlenk tube, to a mixture of 0.96 g of (η^2-dppe)(η^5-C_5Me_5)Fe−C≡C-1,4-$C_6H_4NH_2$ (1.37 mmol) and 1 equiv of 2-pyridinecarboxaldehyde (**6**; 0.13 mL) was added 20 mL of toluene under argon. The solution was refluxed for 5 h, and the solvent was removed from the purple reaction mixture under vacuum. The residue was then washed with *n*-pentane and left under vacuum for 12 h at 50 °C to give 0.80 g of **2** (1.00 mmol) as a dark orange powder. Yield: 73%.

Synthesis of the Complex [Cp*(dppe)Fe−C≡C-1,4-C_6H_4N=CH-2-Py]Cu(PPh_3)Cl (8). A 0.03 g (0.3 mmol) sample of CuCl was added to a boiling solution of 0.24 g (0.3 mmol) of (η^2-dppe)(η^5-C_5Me_5)Fe−C≡C-1,4-C_6H_4N=CH-2-Py (**2**) and 0.08 g (0.3 mmol) of PPh_3 in 20 mL of CH_3CN. The solution was stirred for 20 min. After filtration, the precipitate was washed with *n*-pentane to give the [Cp*(dppe)Fe−C≡C-1,4-C_6H_4N=CH-2-Py]-Cu(PPh_3)Cl complex (**8**) as a blue solid (0.24 g; 0.21 mmol). Yield: 70%. MS (ESI, *m*-NBA): *m*/*z* 1119.2879 ([M−Cl]$^+$, 100%); *m*/*z* calcd for [$C_{68}H_{63}N_2P_3FeCu$] 1119.2849. FT-IR (KBr/Nujol; ν_{max}/cm^{-1}): 2035 (m, C≡C), 1615 (sh, C=N, imine), 1588, 1540 (m, C=N, Py and imine). $^{31}P\{^1H\}$ NMR (81 MHz, $CDCl_3$, H_3PO_4; δ_P): 101.4 (s, 2P, dppe); −4.0 (s, 1P, PPh_3).[19] ^1H NMR (200 MHz, C_6D_6, Me_4Si; δ_H): 8.86 (s, 1H, N=C*H*); 8.50 (d, 1H, J_{HH} = 4.2 Hz, H_6 Py); 8.25 (d, 1H, J_{HH} = 7.2 Hz, H_3 Py); 8.0 (m, 4H, H_o(dppe)); 7.46−6.62 (m, 37H, H_4 Py, H_5 Py, H_{Aryl} and H_{dppe}); 2.67 (m, 2H, PCH_2); 1.85 (m, 2H, PCH_2); 1.55 (s, 15H, C_5Me_5).

Synthesis of the Complex [{Cp*(dppe)Fe−C≡C-1,4-C_6H_4N=CH-2-Py}$_2$Cu][PF_6] (9[PF_6]). In a Schlenk tube, 0.120 g (0.08 mmol) of (η^2-dppe)(η^5-C_5Me_5)Fe−C≡C-1,4-C_6H_4N=CH-2-Py (**2**) and 0.015 g of [(CH_3CN)$_4$Cu][PF_6] (0.04 mmol) were introduced. These solids were dissolved in 20 mL of methanol and stirred overnight at room temperature. The solvent was subsequently evacuated from the dark blue reaction mixture, and the remaining solid was washed with *n*-pentane and dried in vacu*o* to provide the desired complex [{Cp*(dppe)Fe−C≡C-1,4-C_6H_4N=CH-2-Py}$_2$-Cu][PF_6] (**9**[PF_6]) as a deep blue solid (0.058 g; 0.03 mmol). Yield: 80%. Anal. Calcd for $C_{100}H_{96}F_6N_4P_5Fe_2Cu\cdot 2C_5H_{12}$: C, 68.02; H, 6.23 N, 2.88. Found: C, 67.48; H, 5.85; N, 2.78. MS (FAB$^+$, *m*-NBA): *m*/*z* 1651.4580 ([M]$^+$, 100%); *m*/*z* calcd for [$C_{100}H_{96}N_4P_4FeCu$] 1651.4625. FT-IR (KBr; ν_{max}/cm^{-1}): 2029 (m, C≡C), 1995 (sh, C≡C), 1615 (sh, C=N, imine), 1587, 1572 (m, C=N, Py). $^{31}P\{^1H\}$ NMR (81 MHz, $CDCl_3$, H_3PO_4; δ_P): 100.9 (s, 2P, dppe); −142.8 (septuplet, 1P, PF_6). ^1H NMR (200 MHz, $CDCl_3$, Me_4Si; δ_H): 8.71 (broad s, 4H, H_{Py}); 8.17 (broad s, 2H, N=C*H* or H_{Py}), 7.89 (m, 8H, H_{dppe}); 7.60−7.00 (m, 44H, H_{Aryl}, H_{dppe}, and H_{Py}); 6.90 (broad s, 4H, H_{Aryl} or H_{Py}); 2.68 (m, 4H, PCH_2); 1.64 (m, 4H, PCH_2); 1.46 (s, 30H, C_5Me_5). $^{13}C\{^1H\}$ NMR (125 MHz, CD_2Cl_2, Me_4Si; δ_C): 153.5 (broad s, *C*H=N*); 149.4 (s, *C*H$_{Py}$); 142.3 (s, C_{Py}*); 138.0 (s, C_{Ar}); 138.6−134.2−127.0 (*C*H$_{Ar/dppe}$, Fe−*C*≡C, C_{Ar}, and *C*H$_{Py}$); 130.5 (s, *C*H$_{Ar}$) 125.2 (s, *C*H$_{Ar}$); 122.0 (s,

Fe−C≡*C*); 88.0 (s, C_5Me_5); 30.5 (m, CH_2); 9.8 (s, C_5Me_5) (asterisks denote tentative assignments, very weak and broad signals).

ESR Measurements. The Fe(III) complexes were ground with a slight excess of $[(\eta^5\text{-}C_5H_5)_2Fe][PF_6]$ and introduced into a ESR tube under an argon-filled atmosphere. A 1:1 mixture of degassed dichloromethane and 1,2-dichloroethane was transferred to dissolve the solids, just before the mixture was frozen at 80 K and the tube was sealed and transferred to the ESR cavity. The spectra were immediately recorded at that temperature.

Crystallography. Crystals of **2**·$^1/_4CH_2Cl_2$ and **9**$[PF_6]\cdot{}^3/_2CH_2Cl_2$ were obtained as described above. The samples were studied on a NONIUS Kappa CCD with graphite monochromatized Mo Kα radiation. The cell parameters were obtained with Denzo and Scalepack with 10 frames (ψ rotation: 1° per frame).[35] The data collection[36] ($2\theta_{max}$, number of frames, Ω rotation, scan rate, and *hkl* range are given in Table 4) provided reflections for **2**·CH_2Cl_2 and **9**$[PF_6]\cdot 2C_5H_{12}$. Subsequent data reduction with Denzo and Scalepack[35] gave the independent reflections (Table 4). The structures were solved with SIR-97, which revealed the non-hydrogen atoms.[37] After anisotropic refinement, the remaining atoms were found in Fourier difference maps. The complete structures were then refined with SHELXL97[38] by full-matrix least-squares techniques (use of F^2 magnitude; *x*, *y*, *z*, β_{ij} for Fe, P, C, N, and/or O atoms, *x*, *y*, *z* in riding mode for H atoms with variables *N*(var), observations, and *w* used as defined in Table 4). Atomic scattering factors were taken from the literature.[39] ORTEP views of **1**·CH_2Cl_2 and **9**$[PF_6]\cdot 2C_5H_{12}$ were realized with PLATON98.[40]

Acknowledgment. We thank STANDA ATCO (Caen) and the Region Bretagne for financial support.

Supporting Information Available: Figures giving cyclic voltammograms of **2**, **8**, and **9**$[PF_6]$, cyclic voltammograms of [Cu(*N*-Ph,2-Py-aldimine)$_2$]$[PF_6]$ in methanol and dichloromethane, VT $^{31}P\{^1H\}$ NMR spectra of **9**$[PF_6]$, UV−vis spectra of **2**$[PF_6]$, **7**$[PF_6]$, **9**$[PF_6]$, and **9**$[PF_6]_3$, and ESR spectra of **8** and **9**$[PF_6]$ in the presence of excess oxidant and CIF files giving crystallographic data for **2**·$^1/_4CH_2Cl_2$ and **9**$[PF_6]\cdot{}^3/_2CH_2Cl_2$. This material is available free of charge via the Internet at http://pubs.acs.org.

OM061081W

(35) Otwinowski, Z.; Minor, W. In *Methods in Enzymology*; Carter, C. W., Sweet, R. M., Eds.; Academic Press: London, 1997; Vol. 276, pp 307−326.

(36) Kappa CCD Software; Nonius BV, Delft, The Netherlands, 1999.

(37) Altomare, A.; Burla, M. C.; Camalli, M.; Cascarano, G.; Giacovazzo, C.; Guagliardi, A.; Moliterni, A. G. G.; Polidori, G.; Spagna, R. *J. Appl. Chem.* **1998**, *31*, 74−77.

(38) Sheldrick, G. M. SHELX97-2: Program for the Refinement of Crystal Structures; University of Göttingen, Göttingen, Germany, 1997.

(39) *International Tables for X-ray Crystallography*; Kluwer Academic: Dordrecht, The Netherlands, 1992; Vol. C.

(40) Spek, A. L. PLATON: A Multipurpose Crystallographic Tool; Utrecht University, Utrecht, The Netherlands, 1998.